Networks and Heterogeneous Media
Vol. 17, No. 4, August 2022, pp. 593–611
doi:10.3934/nhm.2022018

MODELLING AND NUMERICAL STUDY OF THE POLYATOMIC BITEMPERATURE EULER SYSTEM

Denise Aregba-Driollet and Stéphane Brull*

Univ. Bordeaux, CNRS, Bordeaux INP
IMB, UMR 5251, F-33400 Talence, France

(Communicated by Roberto Natalini)

Abstract. This paper is devoted to the study of the bitemperature Euler system in a polyatomic setting. Physically, this model describes a mixture of one species of ions and one species of electrons in the quasi-neutral regime. We firstly derive the model starting from a kinetic polyatomic model and performing next a fluid limit. This kinetic model is shown to satisfy fundamental properties. Some exact solutions are presented. Finally, a numerical scheme is derived and proved to coincide with an approximation designed in [3] and extended to second order and two space dimensions in [6]. Some numerical tests are presented.

1. **Introduction.** This work is devoted to the modelling and the numerical approximation of the nonconservative polyatomic bitemperature Euler system in the context of plasma physics. Physically, this model describes the interaction of one species of ions and one species of electrons, under the quasi-neutrality assumption.

The aim of this paper is more precisely to provide a construction and an approximation of the polyatomic Euler bitemperature system. This model is constituted of conservative equations for the mass and the momentum and two nonconservative equations for ionic and electronic energies. It is a variant of the system considered in [23]. The nonconservativity is due to source-terms but also to the presence of products of the velocity by pressure gradients. In Inertial Confinement Fusion applications, high temperature solutions involve shocks, for which those nonconservative products have to be determined. This can be done by defining paths, as proposed by Dal Maso, Le Floc'h and Murat ([24]). However, it is shown in [1] that the numerical adaptation of this theory given in [36] is delicate.

In order to compute physically consistent shocks, one can use an underlying kinetic system. This approach was usefully adopted in [3] for the monoatomic case. The model is constituted by a kinetic system coupled with Ampère and Poisson equations. Moreover, this construction leads to a kinetic numerical scheme starting from a semi-discretization in space and time of the kinetic model. A DVM approach of this model has also been considered in [20] together with an asymptotic preserving discretisation toward the bitemperature Euler system. However relaxation schemes and discrete BGK schemes have been developed in the polytropic situation for a

2020 *Mathematics Subject Classification.* Primary: 82C40; Secondary: 76X05, 65M08, 35L60.
Key words and phrases. Nonconservative hyperbolic system, Euler type model for plasmas, BGK model, polyatomic, discrete BGK scheme.

* Corresponding author: Stéphane Brull.

general γ law including the polyatomic case in [3], [6]. It seems important to consider situations where each species has its own γ constant. Note that for smooth solutions, global in time existence has been proved under the condition that these constants are distinct, (see [5]).

We construct in this paper an extension of the model developed in [3] to a polyatomic setting with a continuous energy variable. This model is based on the use of several attractors like in [15] and is shown to satisfy an H theorem. We refer to [10], [13], [14], [19], [11], [34] for other BGK models for polyatomic gas mixtures.

In the present paper, the derivation is based again on an hydrodynamic limit performed from an underlying polyatomic kinetic model. In the present case, the unknowns of the kinetic equations are the distribution functions $f(t, x, v, I)$ depending on time t, space x, velocity v and of one-dimensional internal energy parameter $I > 0$. This energy parameter collects vibrational and rotational energies. Kinetic models with continuous energy variables have been introduced in [16] where the motivation was to develop a Monte-Carlo method. In [17], the authors derived a mesoscopic model of Boltzmann type associated to the previous microscopic model. This collision operator satisfies fundamental properties (H theorem, ...). The generalization to mixtures has been performed in [26]. In [9], a compressible Navier-Stokes model has been derived for mixture of monoatomic and polyatomic gases. For some applications of such models we refer to [35], [38], [29]. In [35] the authors analyse the shock wave structure of some polyatomic gases. So by using an ESBGK model ([2], [21]) they show the presence of a double layer structure that is specific to the polyatomic setting. We mention that in [27], [30], the authors develop polyatomic models with a discrete internal energy variable.

As observed in [37], [3], it is possible to find an underlying kinetic model where the force term is related to the nonconservative terms. One advantage of the kinetic model, is its conservative form. In the present paper, the kinetic model describing the interspecies interaction is a two component polyatomic BGK model based on one continuous internal energy variable coupled with Ampère and Poisson equations. Hence starting from a standard semi-discretization of this model, the hydrodynamic limit leads to a numerical scheme for the bitemperature model. It must be noted that the obtained scheme is the same as the one obtained in section 3.2 of [3]. In this article however the scheme was obtained by a very different method involving models developed in [7] which are not based on a physically realistic kinetic approximation of the equations. The novelty here is that our polyatomic BGK model gives a physical justification to it in the general case where γ_e and γ_i may be distinct. In [4] diffusive terms have been constructed from a Chapman-Enskog expansion up to order 1 leading to a Navier-Stokes type model. This last model generalizes the model that is studied in [22]. In [31], the authors perform a Chapman-Enskog expansion by introducing a small parameter representing the ratio between electronic and ionic molecular masses. They obtain an hyperbolic system with a parabolic regularisation on the electrons. The structure of shock wave solutions for this last model is considered in [39].

The plan of the paper is the following. Section 2 deals with the presentation of the different models that are used in this paper. In particular, we detail the eigenstructure of the bitemperature system. In section 3, the fluid model is obtained starting from the polyatomic model. In section 4 exact solutions for the model are computed and in section 5, the numerical scheme is developed. The last part is devoted to some numerical tests in 1D and 2D configurations.

2. The mathematical models.

2.1. The bitemperature Euler system.

2.1.1. *The fluid model.* The bitemperature Euler system reads

$$\begin{cases} \partial_t \rho + \partial_x(\rho u) = 0, \\ \partial_t(\rho u) + \partial_x(\rho u^2 + p_e + p_i) = 0, \\ \partial_t \mathcal{E}_e + \partial_x(u(\mathcal{E}_e + p_e)) - u(c_i \partial_x p_e - c_e \partial_x p_i) = \nu_{ei}(T_i - T_e), \\ \partial_t \mathcal{E}_i + \partial_x(u(\mathcal{E}_i + p_i)) + u(c_i \partial_x p_e - c_e \partial_x p_i) = -\nu_{ei}(T_i - T_e), \end{cases} \tag{1}$$

where $\rho > 0$ represents the total density of the plasma, u is the average velocity of the plasma, $\mathcal{E}_e$ and $\mathcal{E}_i$ are the total electronic and ionic energies. T_e and T_i represent the electronic and ionic temperatures. The coefficient ν_{ei} is nonnegative. The physically realistic formulas which are given in [33] make the source term very stiff.

One has

$$\rho = \rho_e + \rho_i \tag{2}$$

where $\rho_e = n_e m_e$, $\rho_i = n_i m_i$ are electronic and ionic densities, electronic and ionic concentrations n_e and n_i being assumed to be linked by $Z = n_e/n_i \geq 1$. Z is considered as constant. This situation corresponds to the quasi-neutral regime. m_e and m_i represent the electronic and ionic masses. The mass fractions

$$c_\beta = \frac{\rho_\beta}{\rho}, \quad \beta = e, i \tag{3}$$

are then constant and c_e and c_i are given by

$$c_e = \frac{Z m_e}{m_i + Z m_e}, \quad c_i = 1 - c_e. \tag{4}$$

The total energies are linked to the internal electronic and ionic energies by

$$\mathcal{E}_\beta = \rho_\beta \varepsilon_\beta + \frac{1}{2}\rho_\beta u^2, \quad \beta \in \{e, i\}.$$

The electronic and ionic pressures and temperatures are related by $p_e = n_e k_B T_e$ and $p_i = n_i k_B T_i$. The electronic and ionic internal energies are then given by

$$\varepsilon_e = \frac{k_B}{(\gamma_e - 1)m_e} T_e, \quad \varepsilon_i = \frac{k_B}{(\gamma_i - 1)m_i} T_i,$$

where $\gamma_e, \gamma_i \in [1, 3]$, and k_B is the Boltzmann constant.

In the following we denote $\mathcal{U} = (\rho, \rho u, \mathcal{E}_e, \mathcal{E}_i)$, $U_\beta = (\rho_\beta, \rho_\beta u, \mathcal{E}_\beta)$.

2.1.2. *Hyperbolicity and characteristic fields.* We complete here the calculations presented in [5]. The system is rewritten by using the variables $\mathcal{V} = (\rho, u, \varepsilon_e, \varepsilon_i)$:

$$\begin{cases} \partial_t \rho + u\partial_x \rho + \rho \partial_x u = 0, \\ \partial_t u + u\partial_x u + \rho^{-1}\partial_\rho(p_e + p_i)\partial_x \rho + \rho^{-1}\partial_{\varepsilon_e} p_e \partial_x \varepsilon_e + \rho^{-1}\partial_{\varepsilon_i} p_i \partial_x \varepsilon_i = 0, \\ \partial_t \varepsilon_e + u\partial_x \varepsilon_e + \rho_e^{-1} p_e \partial_x u = \rho_e^{-1}\nu_{ei}(T_i - T_e), \\ \partial_t \varepsilon_i + u\partial_x \varepsilon_i + \rho_i^{-1} p_i \partial_x u = \rho_i^{-1}\nu_{ei}(T_e - T_i). \end{cases} \tag{5}$$

The matrix of the system (5) writes

$$A(\mathcal{V}) = u\, I_4 + \begin{pmatrix} 0 & \rho & 0 & 0 \\ \rho^{-1}\partial_\rho(p_e+p_i) & 0 & \rho^{-1}\partial_{\varepsilon_e} p_e & \rho^{-1}\partial_{\varepsilon_i} p_i \\ 0 & \rho_e^{-1} p_e & 0 & 0 \\ 0 & \rho_i^{-1} p_i & 0 & 0 \end{pmatrix}. \tag{6}$$

We get 4 eigenvalues

$$\lambda_1 = u - a, \quad \lambda_2 = \lambda_3 = u, \quad \lambda_4 = u + a,$$

where

$$a = \sqrt{\sum_{\beta=e,i} \gamma_\beta(\gamma_\beta - 1) c_\beta \varepsilon_\beta}. \tag{7}$$

The value of a given by (7) corresponds to the global sound velocity which yields for the classical Euler system $\sqrt{\gamma p/\rho}$. The eigenvectors associated to the eigenvalue u are equal to

$$r_2 = \begin{pmatrix} 0 \\ 0 \\ -(\gamma_i - 1)c_i \\ (\gamma_e - 1)c_e \end{pmatrix}, \quad r_3 = \begin{pmatrix} -\rho \\ 0 \\ \varepsilon_e \\ \varepsilon_i \end{pmatrix}.$$

This system is then hyperbolic diagonalisable. The fields 2 and 3 are linearly degenerate. Consider now the fields 1 and 4. The eigenvectors are

$$r_1(\mathcal{V}) = \begin{pmatrix} -\rho \\ a \\ -(\gamma_e - 1)\varepsilon_e \\ -(\gamma_i - 1)\varepsilon_i \end{pmatrix}, \quad r_4(\mathcal{V}) = \begin{pmatrix} \rho \\ a \\ (\gamma_e - 1)\varepsilon_e \\ (\gamma_i - 1)\varepsilon_i \end{pmatrix}$$

and

$$\lambda_1'(\mathcal{V}) \cdot r_1(\mathcal{V}) = \lambda_4'(\mathcal{V}) \cdot r_4(\mathcal{V}) = \frac{1}{2a} \sum_{\beta=e,i} (\gamma_\beta(\gamma_\beta - 1)(\gamma_\beta + 1) c_\beta \varepsilon_\beta) > 0. \tag{8}$$

Hence the fields 1 and 4 are genuinely nonlinear.

2.2. **The kinetic model.** In this section, we generalize the BGK model considered in [3] to a polyatomic setting with a continuous energy variable. We firstly precise the notations and next introduce the BGK model that is proved to satisfy the right conservation properties and an H theorem.

2.2.1. *Notations.* Kinetic models for a mixture of two polyatomic gases are described by two distribution functions f_β of species β depending on time $t \in \mathbb{R}^+$, space $x \in \mathbb{R}^3$, velocity $v \in \mathbb{R}^3$ and on internal energy $I \in \mathbb{R}_+$.

Hydrodynamic quantities of species β are defined for $\alpha_\beta \geq 0$ by

$$n_\beta = \int_{\mathbb{R}^3 \times \mathbb{R}_+} f_\beta I^{\alpha_\beta}\, dvdI, \quad u_\beta = \frac{1}{n_\beta} \int_{\mathbb{R}^3 \times \mathbb{R}_+} v f_\beta I^{\alpha_\beta}\, dvdI,$$
$$\mathcal{E}_\beta = \int_{\mathbb{R}^3 \times \mathbb{R}_+} (m_\beta \frac{v^2}{2} + I) f_\beta I^{\alpha_\beta}\, dvdI,$$

and

$$\mathcal{E}_\beta = \frac{1}{2}\rho_\beta u_\beta^2 + \left(\frac{5}{2} + \alpha_\beta\right) n_\beta k_B T_\beta, \quad \beta = e, i.$$

Velocities and temperatures of the mixture u and T are defined by

$$u = \frac{1}{\rho}(\rho_e u_e + \rho_i u_i), \tag{9}$$

$$T = \frac{(\frac{5}{2}+\alpha_e)n_e k_B T_e + (\frac{5}{2}+\alpha_i)n_i k_B T_i + \frac{1}{2}\rho_e u_e^2 + \frac{1}{2}\rho_i u_i^2 - \frac{1}{2}\rho u^2}{(\frac{5}{2}+\alpha_e)n_e k_B + (\frac{5}{2}+\alpha_i)n_i k_B}. \tag{10}$$

The parameters α_e and α_i are related to γ_e and γ_i by the formula ([26])

$$\gamma_e = \frac{1}{\frac{5}{2}+\alpha_e} + 1, \qquad \gamma_i = \frac{1}{\frac{5}{2}+\alpha_i} + 1.$$

For example in the diatomic case, we have $\alpha_e = \alpha_i = 0$. The values $\alpha_e = \alpha_i = -1$ correspond to $\gamma_e = \gamma_i = 5/3$ which is a monoatomic mixture.

Define the entropy of the mixture by

$$\mathcal{H}(f_e, f_i) = \mathcal{H}_s(f_e) + \mathcal{H}_s(f_i), \quad \text{with} \quad \mathcal{H}_s(f_\beta) = \int_{\mathbb{R}^3\times\mathbb{R}_+} (f_\beta\, ln(f_\beta) - f_\beta) I^{\alpha_\beta}\, dvdI \tag{11}$$

and the entropy flux by

$$\Phi(f_e, f_i) = \Phi_s(f_e) + \Phi_s(f_i), \quad \text{with} \quad \Phi_s(f_\beta) = \int_{\mathbb{R}^3\times\mathbb{R}_+} v(f_\beta\, ln(f_\beta) - f_\beta) I^{\alpha_\beta}\, dvdI. \tag{12}$$

2.2.2. *A polyatomic BGK model.* In this section we consider the following kinetic model for $\beta \in \{e; i\}$,

$$\begin{aligned} \partial_t f_\beta(t,x,v,I) &+ v\cdot\nabla_x f_\beta(t,x,v,I) + \frac{q_\beta}{m_\beta} E\cdot\nabla_v f_\beta(t,x,v,I) \\ &= \frac{1}{\tau_\beta}\left(\mathcal{M}_\beta - f_\beta(t,x,v,I)\right) + \frac{1}{\tau_{\beta\delta}}\left(\overline{\mathcal{M}_\beta}(f_e,f_i) - f_\beta(t,x,v,I)\right), \end{aligned} \tag{13}$$

with

$$\mathcal{M}_\beta = \frac{n_\beta}{(2\pi\frac{k_B}{m_\beta}T_\beta)^{\frac{3}{2}}}\frac{1}{\mathcal{Q}_\beta(T_\beta)}\exp\left(-\frac{(v-u_\beta)^2}{2k_B\frac{T_\beta}{m_\beta}} - \frac{I}{k_B T_\beta}\right), \tag{14}$$

$$\overline{\mathcal{M}_\beta}(f_e,f_i) = \frac{n_\beta}{(2\pi\frac{k_B}{m_\beta}T^\#)^{\frac{3}{2}}}\frac{1}{\mathcal{Q}_\beta(T^\#)}\exp\left(-\frac{(v-u^\#)^2}{2k_B\frac{T^\#}{m_\beta}} - \frac{I}{k_B T^\#}\right), \tag{15}$$

where

$$\mathcal{Q}_\beta(T) = \int_0^{+\infty} I^{\alpha_\beta}\exp(-\frac{I}{k_B T})\, dI, \quad \alpha_\beta \geq 0.$$

As suggested in [32] and developed in [3] the definition of $u^\#$ and $T^\#$ as

$$u^\# = \frac{\frac{1}{\tau_{ei}}\rho_e u_e + \frac{1}{\tau_{ie}}\rho_i u_i}{\frac{1}{\tau_{ei}}\rho_e + \frac{1}{\tau_{ie}}\rho_i} \tag{16}$$

and

$$
\begin{aligned}
T^{\#} =& \frac{\frac{1}{\tau_{ei}}(\frac{5}{2}+\alpha_e)n_e k_B T_e + \frac{1}{\tau_{ie}}(\frac{5}{2}+\alpha_i)n_i k_B T_i}{\frac{1}{\tau_{ei}}(\frac{5}{2}+\alpha_e)n_e k_B + \frac{1}{\tau_{ie}}(\frac{5}{2}+\alpha_i)n_i k_B} \\
&+ \frac{1}{2}\frac{\frac{1}{\tau_{ei}}\rho_e u_e^2 + \frac{1}{\tau_{ie}}\rho_i u_i^2 - (\frac{1}{\tau_{ei}}\rho_e + \frac{1}{\tau_{ie}}\rho_i)(u^{\#})^2}{\frac{1}{\tau_{ei}}(\frac{5}{2}+\alpha_e)n_e k_B + \frac{1}{\tau_{ie}}(\frac{5}{2}+\alpha_i)n_i k_B}
\end{aligned}
\tag{17}
$$

gives the conservations of impulsion and total energy for the model (13, 14, 15). These definitions allow in particular to consider a model such that the molecular mass ratios of the species are different. This situation corresponds to the case $\tau_{ei} \neq \tau_{ie}$.

The model (13, 14, 15, 16, 17) is coupled to Ampère and Poisson equations through the electric field E as

$$\partial_t E = -\frac{j}{\varepsilon_0}, \tag{18}$$

$$\nabla_x \cdot E = \frac{\overline{\rho}}{\varepsilon_0}. \tag{19}$$

j represents the plama current, $\overline{\rho}$ the total charge and ε_0 is the permittivity. j and $\overline{\rho}$ are defined by

$$\overline{\rho} = \int_{\mathbb{R}^3\times\mathbb{R}_+} (q_e f_e I^{\alpha_e} + q_i f_i I^{\alpha_i})\, dvdI = n_e q_e + n_i q_i, \tag{20}$$

$$j = \int_{\mathbb{R}^3\times\mathbb{R}_+} v(q_e f_e I^{\alpha_e} + q_i f_i I^{\alpha_i})\, dvdI = n_e q_e u_e + n_i q_i u_i. \tag{21}$$

When one of the two components is monoatomic the model has to be slightly modified. In [8], the authors study for moments systems the link beween polyatomic and monoatomic models. The connexion between monoatomic and polyatomic models can be made by passing to the limit in some parameters. When the two components are monoatomic we refer to [3].

In the case of one monoatomic component and one polyatomic component the model has to be clearly written. Consider for example that electrons are monoatomic whereas ions remain polyatomic. In that case, the model is described with the distributions $f_e(t,x,v)$ and $f_i(t,x,v,I)$. In that case, the model reads

$$
\begin{aligned}
&\partial_t f_e(t,x,v) + v\cdot\nabla_x f_e(t,x,v) + \frac{q_e}{m_e}E\cdot\nabla_v f_e(t,x,v) \\
&\qquad = \frac{1}{\tau_e}\left(\mathcal{M}_e - f_e(t,x,v)\right) + \frac{1}{\tau_{ei}}\left(\overline{\mathcal{M}_e}(f_e,f_i) - f_e(t,x,v)\right),
\end{aligned}
\tag{22}
$$

$$
\begin{aligned}
&\partial_t f_i(t,x,v,I) + v\cdot\nabla_x f_i(t,x,v,I) + \frac{q_i}{m_i}E\cdot\nabla_v f_i(t,x,v,I) \\
&\qquad = \frac{1}{\tau_i}\left(\mathcal{M}_i - f_i(t,x,v,I)\right) + \frac{1}{\tau_{ie}}\left(\overline{\mathcal{M}_i}(f_e,f_i) - f_i(t,x,v,I)\right),
\end{aligned}
\tag{23}
$$

with

$$\mathcal{M}_e = \frac{n_e}{(2\pi\frac{k_B}{m_e}T_e)^{\frac{3}{2}}}\exp\left(-\frac{(v-u_e)^2}{2k_B\frac{T_e}{m_e}}\right), \tag{24}$$

$$\overline{\mathcal{M}_e}(f_e,f_i) = \frac{n_e}{(2\pi\frac{k_B}{m_\alpha}T^{\#})^{\frac{3}{2}}}\exp\left(-\frac{(v-u^{\#})^2}{2k_B\frac{T^{\#}}{m_e}}\right). \tag{25}$$

The hydrodynamic quantities of the monoatomic species are computed as

$$n_e = \int_{\mathbb{R}^3} f_e \, dv, \quad u_e = \frac{1}{n_e} \int_{\mathbb{R}^3} v f_e \, dv, \quad \mathcal{E}_e = \int_{\mathbb{R}^3} m_e \frac{v^2}{2} f_e \, dv.$$

The total impulsion ρu and the total energy $\mathcal{E}$ for the system reads

$$\begin{aligned} \rho u &= \int_{\mathbb{R}^3} m_e v f_e \, dv + \int_{\mathbb{R}^3 \times \mathbb{R}_+} m_i v f_i I^{\alpha_i} \, dv dI, \\ \mathcal{E} &= \int_{\mathbb{R}^3} m_e \frac{v^2}{2} f_e \, dv + \int_{\mathbb{R}^3 \times \mathbb{R}_+} (m_i \frac{v^2}{2} + I) f_i I^{\alpha_i} \, dv dI. \end{aligned}$$

In that case $u^\#$ is given by (16) and $T^\#$ becomes

$$\begin{aligned} T^\# = & \frac{\frac{1}{\tau_{ei}} \frac{3}{2} n_e k_B T_e + \frac{1}{\tau_{ie}} (\frac{5}{2} + \alpha_\beta) n_i k_B T_i}{\frac{1}{\tau_{ei}} \frac{3}{2} n_e k_B + \frac{1}{\tau_{ie}} (\frac{5}{2} + \alpha_i) n_i k_B} \\ & + \frac{1}{2} \frac{\frac{1}{\tau_{ei}} \rho_e u_e^2 + \frac{1}{\tau_{ie}} \rho_i u_i^2 - (\frac{1}{\tau_{ei}} \rho_e + \frac{1}{\tau_{ie}} \rho_i)(u^\#)^2}{\frac{1}{\tau_{ei}} \frac{3}{2} n_e k_B + \frac{1}{\tau_{ie}} (\frac{5}{2} + \alpha_i) n_i k_B}. \end{aligned} \tag{26}$$

As previously, $u^\#$ and $T^\#$ are defined in such a way that the conservation of impulsion and total energy are satisfied. $\mathcal{M}_i$ and $\overline{\mathcal{M}_i}(f_e, f_i)$ are given by (14, 15).

In the present case the definitions of j and $\overline{\rho}$ given in (20, 21) become

$$\begin{aligned} \overline{\rho} &= \int_{\mathbb{R}^3} q_e f_e \, dv + \int_{\mathbb{R}^3 \times \mathbb{R}_+} q_i f_i I^{\alpha_i} \, dv dI, \\ j &= \int_{\mathbb{R}^3} v q_e f_e dv + \int_{\mathbb{R}^3 \times \mathbb{R}_+} v q_i f_i I^{\alpha_i} \, dv dI \end{aligned}$$

and the electric field is still given by (18, 19). For the sake of conciseness, we continue the presentation only for a two polyatomic species mixture. However, the following steps can be easily adapted when one of the components is monoatomic.

2.2.3. *Properties of the model.*

Proposition 1. *The model (13, 14, 15, 16, 17) conserves the mass per species, the total impulsion and the total energy.*

The proof is straighforward and based as in [3] on the definition of the fictitious quantities (16, 17).

Theorem 2.1. *The model (13, 14, 15, 16, 17) satisfies an H theorem. The model satisfies the entropic inequality*

$$\begin{aligned} & \frac{1}{\tau_e} \int_{\mathbb{R}^3 \times \mathbb{R}_+} (\mathcal{M}_e(f_e) - f_e) \ln(f_e) \, I^{\alpha_e} \, dv dI + \frac{1}{\tau_i} \int_{\mathbb{R}^3 \times \mathbb{R}_+} (\mathcal{M}_i(f_i) - f_i) \ln(f_i) \, I^{\alpha_i} \, dv dI \\ & + \frac{1}{\tau_{ei}} \int_{\mathbb{R}^3 \times \mathbb{R}_+} (\overline{\mathcal{M}}_e(f_e, f_i) - f_e) \ln(f_e) \, I^{\alpha_e} \, dv dI \\ & + \frac{1}{\tau_{ie}} \int_{\mathbb{R}^3 \times \mathbb{R}_+} (\overline{\mathcal{M}}_i(f_e, f_i) - f_i) \ln(f_i) \, I^{\alpha_i} \, dv dI \leq 0. \end{aligned}$$

The equality holds in the above equation if and only if there exists $(n_e, n_i, u, T) \in \mathbb{R}_+^2 \times \mathbb{R}^3 \times \mathbb{R}_+$ such that

$$\mathcal{M}_\beta = \frac{n_\beta}{(2\pi \frac{k_B}{m_\beta} T)^{\frac{3}{2}}} \frac{1}{\mathcal{Q}_\beta(T)} \exp\left(- \frac{(v-u)^2}{2 k_B \frac{T}{m_\beta}} - \frac{I}{k_B T} \right), \quad \beta \in \{e, i\}.$$

An important feature of the polyatomic model (13, 14, 15, 16, 17) is that it satisfies an entropy dissipation property that is compatible with the macroscopic one. The entropy dissipation property has already been obtained in [3] for the system (1), starting directly from the fluid system. In the present case, we are able to show that the entropy of the system (1) is compatible with the Boltzmann entropy, see subsection 3.3.

3. Construction of the fluid model.

3.1. Scaling on the one dimensional BGK model.

Suppose that the system (13, 14, 15, 16, 17) is space homogeneous in two directions. So we assume that the system is even in v_2 and v_3. Hence, the distribution function f_β of species β depends on time $t \in \mathbb{R}_+$, space $x \in \mathbb{R}$, velocity $v = (v_1, v_2, v_3)$ and on the energy variable $I \in \mathbb{R}_+$. The model (13, 14, 15, 16, 17) can be rewritten in this case

$$\begin{cases} \partial_t f_\beta + v_1 \partial_x f_\beta + \dfrac{q_\beta}{m_\beta} E \partial_{v_1} f_\beta = \dfrac{1}{\varepsilon}(\mathcal{M}_\beta - f_\beta) + \dfrac{1}{\tau_{\beta\delta}}(\overline{\mathcal{M}_\beta} - f_\beta), \qquad \beta \neq \delta \\ \partial_t E = -\dfrac{j}{\varepsilon^2}, \\ \partial_x E = \dfrac{\overline{\rho}}{\varepsilon^2}, \end{cases} \tag{27}$$

where ε is a nonnegative parameter proportional to the Knudsen number. In that case, Maxwellian distributions (14, 15) become

$$\mathcal{M}_\beta = \frac{n_\beta}{(2\pi \frac{k_B}{m_\beta} T_\beta)^{\frac{3}{2}}} \frac{1}{\mathcal{Q}_\beta(T_\beta)} \exp\left(-\frac{(v_1 - u_\beta)^2 + v_2^2 + v_3^3}{2k_B \frac{T_\beta}{m_\beta}} - \frac{I}{k_B T_\beta} \right), \tag{28}$$

$$\overline{\mathcal{M}_\beta}(f_e, f_i) = \frac{n_\beta}{(2\pi \frac{k_B}{m_\beta} T^\#)^{\frac{3}{2}}} \frac{1}{\mathcal{Q}_\beta(T^\#)} \exp\left(-\frac{(v_1 - u_\beta^\#)^2 + v_2^2 + v_3^2}{2k_B \frac{T^\#}{m_\beta}} - \frac{I}{k_B T^\#} \right) \tag{29}$$

where $u^\#$ and $T^\#$ are defined in (16) and (17).

3.2. Hydrodynamic limit.

Proposition 2. *The system (27, 28, 29, 16, 17) converges formally to the nonconservative bitemperature Euler system where E is given by generalized Ohm's law*

$$\frac{1}{\rho_e}\partial_x p_e - \frac{1}{\rho_i}\partial_x p_i = (\frac{n_e q_e}{\rho_e} - \frac{n_i q_i}{\rho_i})E = \frac{\rho}{\rho_e \rho_i} n_e q_e E = -\frac{\rho}{\rho_e \rho_i} n_i q_i E \tag{30}$$

and

$$\nu_{ei} = \frac{k_B(\frac{5}{2} + \alpha_e)(\frac{5}{2} + \alpha_i) n_e n_i}{\tau_{ie}(\frac{5}{2} + \alpha_e) n_e + \tau_{ei}(\frac{5}{2} + \alpha_i) n_i}. \tag{31}$$

Proof. Performing a Chapman-Enskog expansion, it comes that each component of the species is expanded as

$$f_\beta = \mathcal{M}_\beta + \varepsilon g_\beta, \quad \beta \in \{e, i\} \tag{32}$$

so that

$$\int_{\mathbb{R}^3 \times \mathbb{R}_+} g_\beta \, I^{\alpha_\beta} \, dvdI = 0, \quad \int_{\mathbb{R}^3 \times \mathbb{R}_+} v_1 \, g_\beta \, I^{\alpha_\beta} \, dvdI = 0, \tag{33}$$

$$\int_{\mathbb{R}^3 \times \mathbb{R}_+} (\frac{1}{2} m_\beta v^2 + I) g_\beta I^{\alpha_\beta} \, dvdI = 0. \tag{34}$$

Moreover, Gauss equation in (27) implies that $n_i q_i = -n_e q_e + \mathcal{O}(\varepsilon^2)$. So, $n_e = Z n_i + \mathcal{O}(\varepsilon^2)$. Ampère equation then gives $u_e = u_i + \mathcal{O}(\varepsilon^2) = u$. Plugging (32) into the first equation of (27) leads to

$$\partial_t \mathcal{M}_\beta + v_1 \partial_x \mathcal{M}_\beta + \frac{q_\beta}{m_\beta} E \partial_{v_1} \mathcal{M}_\beta = -g_\beta + \frac{1}{\tau_{\beta\delta}} (\overline{\mathcal{M}}_\beta - \mathcal{M}_\beta) + \mathcal{O}(\varepsilon) \tag{35}$$

for $\{\beta;\, \delta\} \in \{e; i\}, \quad \beta \neq \delta$.

Mass conservation equation is obtained by integrating w.r.t v and I. The equation of the conservation of the impulsion is then recovered by taking the second moment of (35). Moreover, proceeding as in [3], we get Ohm's law (30). Next the energy equation on the electrons writes

$$\begin{aligned}
&\int_{\mathbb{R}^3 \times \mathbb{R}_+} (\partial_t \mathcal{M}_e + v_1 \partial_x \mathcal{M}_e)(\frac{1}{2} m_e v^2 + I) I^{\alpha_e}\, dv dI \\
&+ \int_{\mathbb{R}^3 \times \mathbb{R}_+} \frac{q_e}{m_\beta} E \partial_{v_1} \mathcal{M}_e\, (\frac{1}{2} m_e v^2 + I) I^{\alpha_e}\, dv dI \\
&= \frac{1}{\tau_{ei}} \int_{\mathbb{R}^3 \times \mathbb{R}_+} (\overline{\mathcal{M}}_e - \mathcal{M}_e)\, (\frac{1}{2} m_e v^2 + I) I^{\alpha_e}\, dv dI.
\end{aligned}$$

Moreover a direct computation gives

$$\int_{\mathbb{R}^3 \times \mathbb{R}_+} (\overline{\mathcal{M}}_e - \mathcal{M}_e)\, (\frac{1}{2} m_e v^2 + I) I^{\alpha_e}\, dv dI = (\frac{5}{2} + \alpha_e) n_e k_B (T^{\#} - T_e).$$

So, according to the relation (10) defining T, we get

$$\begin{aligned}
&\int_{\mathbb{R}^3 \times \mathbb{R}_+} (\overline{\mathcal{M}}_e - \mathcal{M}_e)\, (\frac{1}{2} m_e v^2 + I) I^{\alpha_e}\, dv dI \\
&\qquad = \frac{(\frac{5}{2} + \alpha_e) n_e\, (\frac{5}{2} + \alpha_i) n_i}{\tau_{ie} (\frac{5}{2} + \alpha_e) n_e + \tau_{ei} (\frac{5}{2} + \alpha_i) n_i} k_B (T_i - T_e)
\end{aligned}$$

and ν_{ei} is given by (31). □

3.3. **Entropy dissipation.** As proved in [3], the system (1) owns a dissipative entropy-entropy flux pair

$$\eta = \eta_e + \eta_i, \quad Q = u\, \eta \tag{36}$$

where

$$\eta_\beta = -\frac{\rho_\beta}{m_\beta (\gamma_\beta - 1)} \left[\ln \left(\frac{(\gamma_\beta - 1) \rho_\beta \varepsilon_\beta}{\rho_\beta^{\gamma_\beta}} \right) + C \right], \quad \beta = e, i. \tag{37}$$

Here, C is a nonegative constant. With the same method as in [3] we can prove

Theorem 3.1. *Let (η, Q) be defined by (36)-(37). η is a strictly convex dissipative entropy for system (1) and Q is the related entropy flux. More precisely, any smooth solution of the system satisfies the following equality:*

$$\partial_t \eta(\mathcal{U}) + \partial_x Q(\mathcal{U}) = -\frac{\nu_{ei}}{k_B T_i T_e} (T_i - T_e)^2. \tag{38}$$

If $\mathcal{U}$ is a weak solution of system (1) obtained as the hydrodynamic limit of the kinetic model, then it satisfies the following inequality

$$\partial_t \eta(\mathcal{U}) + \partial_x Q(\mathcal{U}) \leq -\frac{\nu_{ei}}{k_B T_i T_e} (T_i - T_e)^2. \tag{39}$$

As in [3], the inequality (39) is obtained by using the proof of the H theorem (Theorem 2.1).

4. **Some exact solutions.** We compute contact discontinuities and rarefaction waves for system (1) in the homogeneous case $\nu_{ei} = 0$. As u is a double eigenvalue we have contact discontinuities of two kinds. Moreover the computation of the rarefaction waves is different from the one for the classical Euler system.

4.1. **Contact discontinuities.** A contact discontinuity is a weak solution $\mathcal{U} = (\rho, \rho u, \mathcal{E}_e, \mathcal{E}_i)$ of (1) such that u is a constant and

$$\rho(x,t) = \begin{vmatrix} \rho_L \text{ if } x < ut, \\ \rho_R \text{ if } x > ut \end{vmatrix} \quad \mathcal{E}_\beta(x,t) = \begin{vmatrix} \mathcal{E}_{\beta,L} \text{ if } x < ut, \\ \mathcal{E}_{\beta,R} \text{ if } x > ut \end{vmatrix} \quad \beta = e, i.$$

Here, ρ_L, ρ_R, $\mathcal{E}_{\beta,L}$, $\mathcal{E}_{\beta,R}$ are constant. In that case the homogeneous system related to (1) can be written under the conservative form:

$$\begin{cases} \partial_t \rho + \partial_x(\rho u) = 0, \\ \partial_t(\rho u) + \partial_x(\rho u^2 + p_e + p_i) = 0, \\ \partial_t \mathcal{E}_e + \partial_x(u(\mathcal{E}_e + c_e(p_e + p_i))) = 0, \\ \partial_t \mathcal{E}_i + \partial_x(u(\mathcal{E}_i + c_i(p_e + p_i))) = 0. \end{cases} \tag{40}$$

Rankine-Hugoniot jump conditions are

$$[u] = 0, \quad [p_e + p_i] = 0.$$

One can realize those conditions by taking $[\rho] = 0$ or not. In the first case, nontrivial contact discontinuities are obtained with nonequal left and right values of the ionic and electronic pressures. This case is specific to the bitemperature model. The case $[\rho] \neq 0$ appears also in contact discontinuities for the 3×3 monotemperature Euler system.

For contact discontinuities there is no entropy dissipation:

$$\partial_t \eta(\mathcal{U}) + \partial_x Q(\mathcal{U}) = 0.$$

4.2. **Rarefaction waves.** A rarefaction wave is a selfsimilar continuous, piecewise C^1 solution of (1) with $\nu_{ei} = 0$. As we look for a smooth solution, we may use the variable $\mathcal{V} = (\rho, u, \varepsilon_e, \varepsilon_i)$. The rarefaction waves are given by solutions $\mathcal{V}(x,t) = \mathcal{W}\left(\frac{x}{t}\right)$ of the homogeneous system related to (5) that is, denoting $y = x/t$:

$$\{-y\, I \, + A\,(\mathcal{W}\,(y))\}\, \mathcal{W}'(y) = 0 \tag{41}$$

where A is given by (6). Rarefaction waves are closely related to the integral curves of the eigenvectors of A, as soon as the fields are genuinely nonlinear, see [18] for example. Let us consider the eigenvalue $\lambda_+ = u + a$ with a given by (7), with the eigenvector r_4 satisfying (8). We solve the ODS

$$\Phi'(\xi) = r_4(\Phi(\xi)), \quad \Phi(0) = \mathcal{W}_L.$$

We set $\mathcal{W}_R = \Phi(\xi_0)$ with $\xi_0 > 0$ and $\Psi(\xi) = \lambda_+(\Phi(\xi))$. Ψ is an increasing monotone function. We set

$$\mathcal{W}(y) = \begin{vmatrix} \mathcal{W}_L & si \;\; y \leq \lambda_+(\mathcal{W}_L), \\ \Phi(\Psi^{-1}(y)) & \text{if } \; \lambda_+(\mathcal{W}_L) \leq y \leq \lambda_+(\mathcal{W}_R), \\ \mathcal{W}_R & si \;\; y \geq \lambda_+(\mathcal{W}_R). \end{vmatrix}$$

We have $\mathcal{W} \in C^0(\mathbb{R})$ and (41). Hence we have to solve for $\xi > 0$:

$$\begin{cases} \rho'(\xi) &= \rho(\xi), \\ u'(\xi) &= a(\xi), \\ \varepsilon'_\beta(\xi) &= (\gamma_\beta - 1)\varepsilon_\beta(\xi), \quad \beta = e, i. \end{cases} \qquad (\rho(0), u(0), \varepsilon_e(0), \varepsilon_i(0)) = \mathcal{W}_L \,.$$

We find

$$\begin{cases} \rho(\xi) &= \rho_L \mathrm{e}^{\xi}\,, \\ u'(\xi) &= \sqrt{\displaystyle\sum_\beta \gamma_\beta(\gamma_\beta - 1) c_\beta \varepsilon_{\beta,L} \mathrm{e}^{(\gamma_\beta - 1)\xi}}\,, \\ \varepsilon_\beta(\xi) &= \varepsilon_{\beta,L} \mathrm{e}^{(\gamma_\beta - 1)\xi}\,, \quad \beta = e, i. \end{cases} \qquad (42)$$

As

$$T_\beta = \frac{(\gamma_\beta - 1) m_\beta}{k_B} \varepsilon_\beta \quad \text{and} \quad p_\beta = (\gamma_\beta - 1)\rho_\beta \varepsilon_\beta,$$

we have also:

$$T_\beta(\xi) = T_{\beta,L} \mathrm{e}^{(\gamma_\beta - 1)\xi} \quad \text{et} \quad p_\beta(\xi) = p_{\beta,L} \mathrm{e}^{\gamma_\beta \xi}\,, \quad \beta = e, i.$$

If $\gamma_i \neq \gamma_e$ we cannot parametrize the rarefaction curves by the pressure as one does for the monotemperature Euler system. Hence from (42), the rarefaction curves can be parametrized as follows

$$\xi = \ln\left(\frac{\rho}{\rho_L}\right), \quad \varepsilon_\beta = \varepsilon_{\beta,L}\left(\frac{\rho}{\rho_L}\right)^{\gamma_\beta - 1}.$$

So

$$T_\beta = T_{\beta,L}\left(\frac{\rho}{\rho_L}\right)^{\gamma_\beta - 1}.$$

We retrieve the fact that $\rho_R > \rho_L$. We have also $p_\beta > p_{\beta,L}$ and the specific entropy by species is constant. It is defined by

$$S_\beta = \frac{p_\beta}{\rho_\beta^{\gamma_\beta}}\,.$$

For all ξ:

$$S_\beta(\xi) = S_\beta(0), \quad \beta = e, i$$

hence

$$S_{\beta,L} = S_{\beta,R}, \quad \beta = e, i.$$

5. **Numerical approximation.** In this section we derive a numerical scheme starting from a semi-discretization of the kinetic model. In [3], this approach has been developed for a monoatomic gas mixture. We follow the lines of [3] and obtain the scheme for the polyatomic case. For the sake of completeness we give the details.

First we recall that for P_β defined by

$$P_\beta(f_\beta) = \int_{\mathbb{R}^3 \times \mathbb{R}_+} \begin{pmatrix} m_\beta \\ m_\beta v_1 \\ (m_\beta \frac{v^2}{2} + I) \end{pmatrix} f_\beta \, I^{\alpha_\beta} dv dI \qquad (43)$$

one has

$$P_\beta(f_\beta^n) = U_{\beta,j}^n, \quad P_\beta\left(v_1 \mathcal{M}_\beta(U_{\beta,j}^n)\right) = F_\beta(U_{\beta,j}^n), \qquad (44)$$

where F_β is the flux of 3×3 Euler equations with γ_β pressure law.

The spatial discretisation is defined by the step Δx and the cells $C_j =]x_{j-\frac{1}{2}}, x_{j+\frac{1}{2}}[$. We consider that Δx is constant whereas the time step Δt: $t_0 = 0$, $t_{n+1} = t_n + \Delta t$ can be variable.

We use a finite volume approach: for any unknown $V(x,t)$, we look for the approximation V_j^n of the average of V at time t_n on the cell C_j. Suppose that $\mathcal{U}^n$ is known ($n \geq 0$).

First step. For $\beta = e, i$ we set

$$\rho_{\beta,j}^n = c_\beta \rho_j^n \tag{45}$$

and $U_{\beta,j}^n = (\rho_{\beta,j}^n, \rho_{\beta,j}^n u_j^n, \mathcal{E}_{\beta,j})$. $f_e^n(v,I)$, $f_i^n(v,I)$ are computed by projection on the maxwellian states:

$$\forall j, \quad f_{\beta,j}^n(v,I) = \mathcal{M}_\beta(U_{\beta,j}^n, v, I), \quad \beta = e,\, i. \tag{46}$$

Second step. We solve the transport equations $\partial_t f_\beta + v_1 \partial_x f_\beta = 0$ by using a numerical flux $h_{\beta,j+\frac{1}{2}}(v,I) = h_\beta(f_{\beta,j}(v,I), f_{\beta,j+1}(v,I), v, I)$. Here we choose the HLL type flux

$$h_\beta(f,g,v,I) = v_1 \left(\frac{\lambda_2}{\lambda_2 - \lambda_1} f(v,I) - \frac{\lambda_1}{\lambda_2 - \lambda_1} g(v,I) \right) + \frac{\lambda_1 \lambda_2}{\lambda_2 - \lambda_1} (g(v,I) - f(v,I)), \tag{47}$$

where $\lambda_1 \leq 0 \leq \lambda_2$ are distinct real constants to be fixed. We set for all (v,I)

$$f_{\beta,j}^{n+\frac{1}{2}}(v,I) = f_{\beta,j}^n(v,I) - \frac{\Delta t}{\Delta x} \left(h_{\beta,j+\frac{1}{2}}^n(v,I) - h_{\beta,j-\frac{1}{2}}^n(v,I) \right).$$

Remark 1. This scheme is stable for $\lambda_1 \leq v_1 \leq \lambda_2$ and appropriate CFL condition. As we are going to integrate this formula w.r.t. $v_1 \in \mathbb{R}$, we have no chance to prove stability at this level. The resulting macroscopic scheme owns however stability properties that can be proven by a different way, as we shall show at the end of this section.

We apply P_e on f_e, P_i on f_i, and obtain $U_{e,j}^{n+\frac{1}{2}}$ and $U_{i,j}^{n+\frac{1}{2}}$:

$$U_{\beta,j}^{n+\frac{1}{2}} = P_\beta(f_{\beta,j}^{n+\frac{1}{2}}) = \begin{pmatrix} \rho_{\beta,j}^{n+\frac{1}{2}} \\ \rho_{\beta,j}^{n+\frac{1}{2}} u_{\beta,j}^{n+\frac{1}{2}} \\ \mathcal{E}_{\beta,j}^{n+\frac{1}{2}} \end{pmatrix}$$

Denoting for $\beta = e, i$

$$F_{\beta,j+\frac{1}{2}} = \mathcal{F}_\beta(U_{\beta,j}, U_{\beta,j+1}), \quad \mathcal{F}_\beta(U_\beta, V_\beta) = P_\beta(h_\beta(\mathcal{M}_\beta(U_\beta), \mathcal{M}_\beta(V_\beta), \cdot)), \tag{48}$$

we have by using (44), (46) and (47)

$$\mathcal{F}_\beta(U_\beta, V_\beta) = \frac{\lambda_2}{\lambda_2 - \lambda_1} F_\beta(U_\beta) - \frac{\lambda_1}{\lambda_2 - \lambda_1} F_\beta(V_\beta) + \frac{\lambda_1 \lambda_2}{\lambda_2 - \lambda_1} (V_\beta - U_\beta),$$

and

$$U_{\beta,j}^{n+\frac{1}{2}} = U_{\beta,j}^n - \frac{\Delta t}{\Delta x} \left(F_{\beta,j+\frac{1}{2}}^n - F_{\beta,j-\frac{1}{2}}^n \right).$$

Hence $U_{\beta,j}^{n+\frac{1}{2}}$ is computed by the HLL scheme ($\lambda_1 \leq 0 \leq \lambda_2$).

Remark 2. We could have chosen the upwind scheme to approximate the transport equations, but it is more difficult to integrate the formulas w.r.t. v_1 in this case, because the numerical flux depends on the sign of v_1.

It is easy to prove the following result.

Proposition 3. *For $\beta = e, i$*

$$\rho_{\beta,j}^{n+\frac{1}{2}} = c_\beta \rho_j^{n+\frac{1}{2}} \tag{49}$$

where ρ is defined in (2).

Third step. We take into account the force terms and the source terms. For all $j \in \mathbb{Z}$, $\alpha, \beta \in \{e, i\}$ and $\beta \neq \alpha$, we define

$$f_{\beta,j}^{n+\frac{3}{4}}(v, I) = f_{\beta,j}^{n+\frac{1}{2}} - \Delta t \frac{q_\beta}{m_\beta} E_j^{n+1} \nabla_v f_{\beta,j}^{n+\frac{3}{4}} + \frac{\Delta t}{\tau_{\beta\delta}} \left(\overline{\mathcal{M}_\beta} \left(f_{e,j}^{n+\frac{3}{4}}, f_{i,j}^{n+\frac{3}{4}} \right) - f_{\beta,j}^{n+\frac{3}{4}} \right) \tag{50}$$

and

$$U_{\beta,j}^{n+1} = P_\beta(f_{\beta,j}^{n+\frac{3}{4}}). \tag{51}$$

One obtains the following equations for $\beta = e, i$:

$$\begin{cases} \rho_{\beta,j}^{n+1} & = c_\beta \rho_j^{n+\frac{1}{2}} \\ \rho_{\beta,j}^{n+1} u_{\beta,j}^{n+1} & = \rho_{\beta,j}^n u_{\beta,j}^n - \dfrac{\Delta t}{\Delta x} \left(F_{\beta,j+\frac{1}{2},2}^n - F_{\beta,j-\frac{1}{2},2}^n \right) - \dfrac{\Delta t\, q_\beta}{m_\beta} E_j^{n+1} \rho_{\beta,j}^{n+1} \\ \mathcal{E}_{\beta,j}^{n+1} & = \mathcal{E}_{\beta,j}^n - \dfrac{\Delta t}{\Delta x} \left(F_{\beta,j+\frac{1}{2},3}^n - F_{\beta,j-\frac{1}{2},3}^n \right) \\ & \quad - E_j^{n+1} u_{\beta,j}^{n+1} \dfrac{\Delta t\, q_\beta}{m_\beta} \rho_{\beta,j}^{n+1} + \Delta t \nu^{ei} (T_{\beta',j}^{n+1} - T_{\beta,j}^{n+1}), \quad \beta' \neq \beta. \end{cases} \tag{52}$$

Subsequently, it is necessary to ensure that the quasineutrality constraints are satisfied, which correspond to Maxwell-Gauss and Maxwell-Ampère equations in the limit $\varepsilon \to 0$:

$$\frac{q_e}{m_e} \rho_{e,j}^{n+1} + \frac{q_i}{m_i} \rho_{i,j}^{n+1} = 0, \quad \frac{q_e}{m_e} \rho_{e,j}^{n+1} u_{e,j}^{n+1} + \frac{q_i}{m_i} \rho_{i,j}^{n+1} u_{i,j}^{n+1} = 0.$$

By proposition 3 the first condition is satisfied and $\rho_j^{n+1} = \rho_j^{n+\frac{1}{2}}$. The second condition is equivalent to $u_{i,j}^{n+1} = u_{e,j}^{n+1} = u_j^{n+1}$. As a consequence if $\mathcal{U}_j^{n+1} = (\rho_j^{n+1}, \rho_j^{n+1} u_j^{n+1}, \mathcal{E}_{e,j}^{n+1}, \mathcal{E}_{i,j}^{n+1})$ then $U_{e,j}^{n+1}$ and $U_{i,j}^{n+1}$ satisfy (45), so our notation is consistent. By applying these properties to (52) for $\beta = e, i$, one gets:

$$\begin{aligned} c_e \rho_j^{n+1} u_j^{n+1} &= c_e \rho_j^n u_j^n - \frac{\Delta t}{\Delta x} \left(F_{e,j+\frac{1}{2},2}^n - F_{e,j-\frac{1}{2},2}^n \right) - \frac{\Delta t\, q_e}{m_e} E_j^{n+1} \rho_{e,j}^{n+1}, \\ c_i \rho_j^{n+1} u_j^{n+1} &= c_i \rho_j^n u_j^n - \frac{\Delta t}{\Delta x} \left(F_{i,j+\frac{1}{2},2}^n - F_{j-\frac{1}{2},2}^{i,n} \right) - \frac{\Delta t\, q_i}{m_i} E_j^{n+1} \rho_{i,j}^{n+1}. \end{aligned}$$

Hence, by multiplying the first equation by c_i and the second equation by c_e, and then by substracting one to the other, one obtains, analoguously to the continuous case, the discrete generalized Ohm law:

$$E_j^{n+1} \frac{q_i}{m_i} \rho_{i,j}^{n+1} = -E_j^{n+1} \frac{q_e}{m_e} \rho_{e,j}^{n+1} = \frac{1}{\Delta x} (\delta_{j+\frac{1}{2}}^n - \delta_{j-\frac{1}{2}}^n),$$

where

$$\delta_{j+\frac{1}{2}}^n = -c_i F_{e,j+\frac{1}{2},2}^n + c_e F_{i,j+\frac{1}{2},2}^n. \tag{53}$$

Finally, defining $F_{j+\frac{1}{2}}$ by

$$F_{j+\frac{1}{2}} = \begin{pmatrix} F_{e,j+\frac{1}{2},1} + F_{i,j+\frac{1}{2},1} \\ F_{e,j+\frac{1}{2},2} + F_{i,j+\frac{1}{2},2} \\ F_{e,j+\frac{1}{2},3} \\ F_{i,j+\frac{1}{2},3} \end{pmatrix}, \tag{54}$$

we get a scheme that is consistent with the Euler system (1):

Proposition 4. *For any $n \geq 0$ if $\mathcal{U}^n = \{\mathcal{U}_j^n\}_{j\in\mathbb{Z}}$ is the approximate solution of the system (1) at time t_n, we set*

$$U_{\beta,j}^n = (c_\beta \rho_j^n, c_\beta \rho_j^n u_j^n, \mathcal{E}_\beta), \quad \beta = e, i. \tag{55}$$

The kinetic flux h_β is defined by (47). The numerical fluxes $F_{\beta,j+\frac{1}{2}}$, $\delta_{j+\frac{1}{2}}$ and $F_{j+\frac{1}{2}}$ are then defined by (48), (53), (54). The approximate solution at time t_{n+1} is defined by the implicit scheme

$$\begin{cases} \rho_j^{n+1} = \rho_j^n - \dfrac{\Delta t}{\Delta x}\left(F_{j+\frac{1}{2},1}^n - F_{j-\frac{1}{2},1}^n\right), \\ \rho_j^{n+1} u_j^{n+1} = \rho_j^n u_j^n - \dfrac{\Delta t}{\Delta x}\left(F_{j+\frac{1}{2},2}^n - F_{j-\frac{1}{2},2}^n\right), \\ \mathcal{E}_{e,j}^{n+1} = \mathcal{E}_{e,j}^n - \dfrac{\Delta t}{\Delta x}\left(F_{e,j+\frac{1}{2},3}^n - F_{e,j-\frac{1}{2},3}^n\right) - u_j^{n+1}\dfrac{\Delta t}{\Delta x}\left(\delta_{j+\frac{1}{2}}^n - \delta_{j-\frac{1}{2}}^n\right) \\ \qquad + \Delta t \nu_{ei}(T_{i,j}^{n+1} - T_{e,j}^{n+1}), \\ \mathcal{E}_{i,j}^{n+1} = \mathcal{E}_{i,j}^n - \dfrac{\Delta t}{\Delta x}\left(F_{i,j+\frac{1}{2},3}^n - F_{i,j-\frac{1}{2},3}^n\right) + u_j^{n+1}\dfrac{\Delta t}{\Delta x}\left(\delta_{j+\frac{1}{2}}^n - \delta_{j-\frac{1}{2}}^n\right) \\ \qquad - \Delta t \nu_{ei}(T_{i,j}^{n+1} - T_{e,j}^{n+1}). \end{cases} \tag{56}$$

Remark 3. The scheme is implicit but easy to implement because the first two equations of (56) give ρ_j^{n+1} and u_j^{n+1} explicitly and the two last equations can be expressed as a linear 2×2 system for the unknown T_e, T_i.

This numerical scheme is the same as the one obtained in section 3.2 of [3] and for which a second order two-dimensional extension is presented in [6], ($\lambda_1\lambda_2 \leq 0$). However, in these two articles, the scheme was obtained by a very different method involving models developed in [7]. Those models are formally like discrete BGK equations but are not based on a physically realistic kinetic representation of the equations. The novelty here is that our polyatomic BGK model gives a physical justification to it, including the case $\gamma_e \neq \gamma_i$.

We recall that stability and entropy properties where proved in these references. In particular, a discrete entropy inequality holds under appropriate choices of λ_1 and λ_2 and a CFL condition using the sound velocity of each species. These theoritical conditions give rise however to too much numerical diffusion. We replace them by using the global sound velocity defined in (7) (see [6]):

$$\lambda_1 \leq \min(u-a) \leq \max(u+a) \leq \lambda_2, \quad \max(|\lambda_1|, |\lambda_2|)\frac{\Delta t}{\Delta x} \leq 1. \tag{57}$$

6. **Numerical results.** As pointed out in section 5, the presented scheme has already been tested in [3] and [6]. The aim of this section is to investigate more precisely the polyatomic case with two tests where $\gamma_e = \frac{5}{3}$ and $\gamma_i = \frac{7}{5}$. We make use of the second order extension in space and time with affine reconstruction and Heun scheme developed in [6].

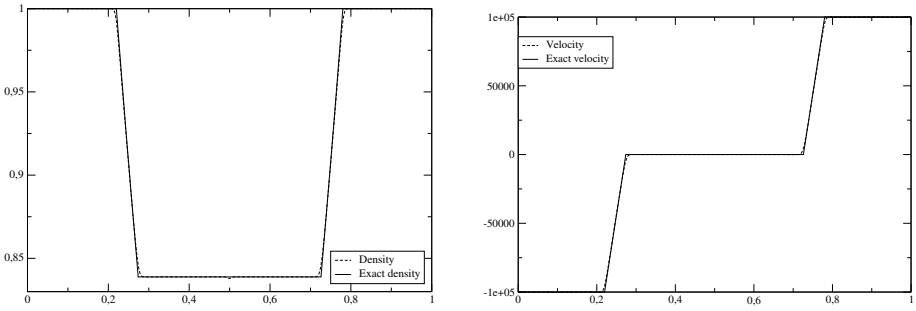

FIGURE 1. Double rarefaction. Left: density. Right: velocity.

6.1. **Double rarefaction.** We solve the bitemperature Euler system with the following Riemann data, whose orders of magnitude are those encountered in physical situations:

$$\rho_- = 1, \qquad \rho_+ = \rho_-, \qquad u_- = -100000, \qquad u_+ = -u_-,$$
$$T_{e,-} = 2.3 \times 10^7, \quad T_{e,+} = T_{e,-}, \quad T_{i,-} = 2.3 \times 10^6, \quad T_{i,+} = T_{i,-}.$$

We set $Z = 1$ and a final computation time $t = 4.0901 \times 10^{-7}\, sec.$ The numerical simulations are performed on the interval $[0, 1]$ with 2000 cells. The values of λ_1 and λ_2 are computed at every time-step with the condition (57). We set $\nu_{ei} = 0$ so that the solution consists of two rarefaction waves propagating to left and right, the contact discontinuity being trivial. In order to determine the analytical solution, denoting $(\rho, u, \varepsilon_e, \varepsilon_i)$ the intermediate state, one has to find $\xi > 0$ such that:

$$\begin{cases} \rho = \rho_\pm \mathrm{e}^{-\xi} \\ u = u_- + \displaystyle\int_0^\xi a(s)ds = u_+ - \int_0^\xi a(s)ds \\ \varepsilon_\beta = \mathrm{e}^{-(\gamma_\beta - 1)\xi} \varepsilon_{\beta,\pm}, \quad \beta = e, i, \end{cases}$$

with

$$a(s) = \left(\sum_\beta \gamma_\beta(\gamma_\beta - 1) c_\beta \varepsilon_{\beta,\pm} \mathrm{e}^{-(\gamma_\beta - 1)s} \right)^{1/2}.$$

Hence we find numerically $\xi > 0$ such that

$$u_+ = \int_0^\xi a(s)ds.$$

The numerical results are depicted in Figures 1 and 2. We compare the exact and computed results for density, velocity and temperatures. As already observed in [3] for $\gamma_e = \gamma_i = 5/3$, a peak of ionic temperature happens at $x = 1/2$. This peak is similar as the one observed classically for the monotemperature 3×3 Euler system.

6.2. **Two dimensional implosion.** In this test case, we consider an implosion problem, introduced in [28] in the monoatomic case $\gamma_e = \gamma_i = \frac{5}{3}$. We compared our approach with the conservative one of this paper in [6]. Here we set $\gamma_e = \frac{5}{3}$ and $\gamma_i = \frac{7}{5}$ and keep the other parameters unchanged, that is: the physical domain

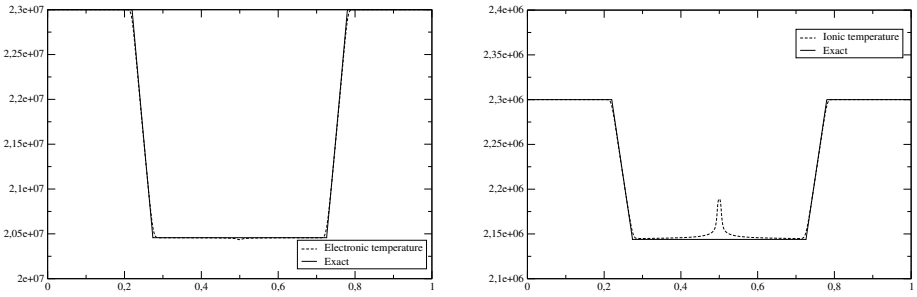

FIGURE 2. Double rarefaction. Left: electronic temperature. Right : ionic temperature.

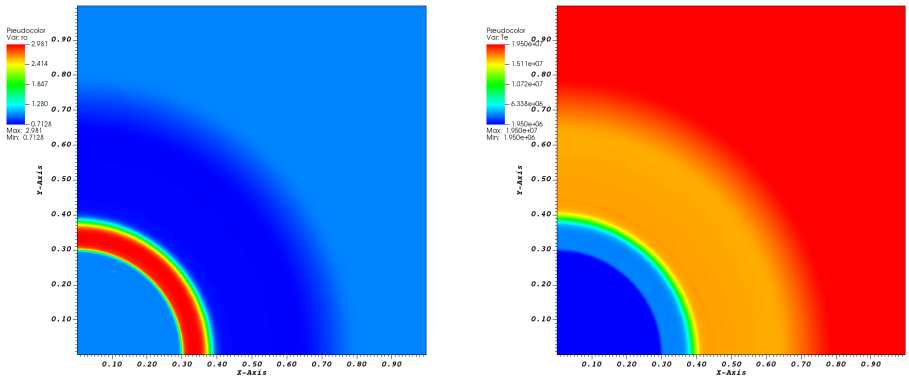

FIGURE 3. Total density (left) and electronic temperature (right) at time $t = 4.0901 \times 10^{-7}$s for an implosion test case with ν_{ei} given by the NRL formulary with a grid of 500 by 500 points.

is the square $[-1,1] \times [-1,1]$. Initial data for this Riemann problem is as follows: $\rho = 1$ kg.m^{-3}, $u = 0$ m.s^{-1} and temperatures are given by:

$$T^e(x_1,x_2,0) = 2,3 \times 10^6 K, \quad T^i(x_1,x_2,0) = 1.7406 \times 10^6 K \quad \text{if } (x_1)^2 + (x_2)^2 < \frac{1}{4},$$
$$T^e(x_1,x_2,0) = 2,3 \times 10^7 K, \quad T^i(x_1,x_2,0) = 1.7406 \times 10^7 K \quad \text{otherwise.}$$

The relaxation frequency ν_{ei} is chosen realistically, according to the formulae given by the NRL formulary [33]. Due to stiffness of the source term one has $T_e = T_i$ very quickly.

Thanks to symmetry properties of the problem, it is only necessary to solve it on the quarter domain $[0,1] \times [0,1]$, equipped with suitable boundary conditions.

On Figure 3, are given the isovalues of the total density and of the electronic temperature at time $t = 4.0901 \times 10^{-7}$ sec. We can see that the qualitative behaviour is the same as in the monoatomic case, see Figure 7 of [6]. Here also one can observe a shock propagating towards the center of the domain, a contact discontinuity, and a rarefaction wave propagating to the exterior. However the values of densities and temperatures are different.

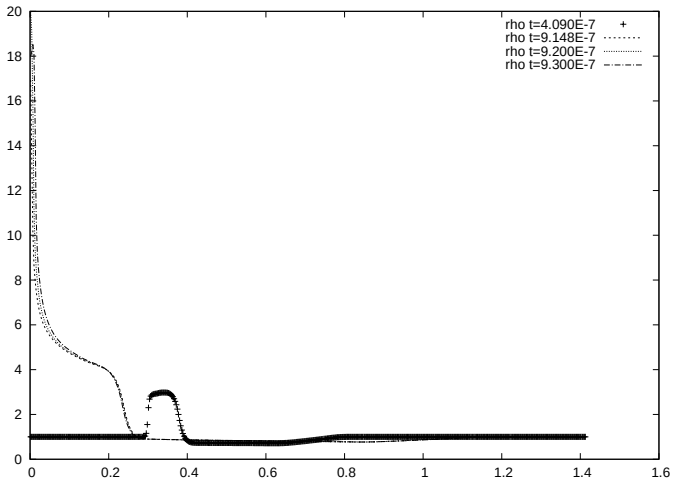

FIGURE 4. Implosion test case with ν_{ei} given by the NRL formulary with a grid of 500 by 500 points. Density along the first bisector at 4 different times: the peak occurs for $t = 9.2 \times 10^{-7}$sec.

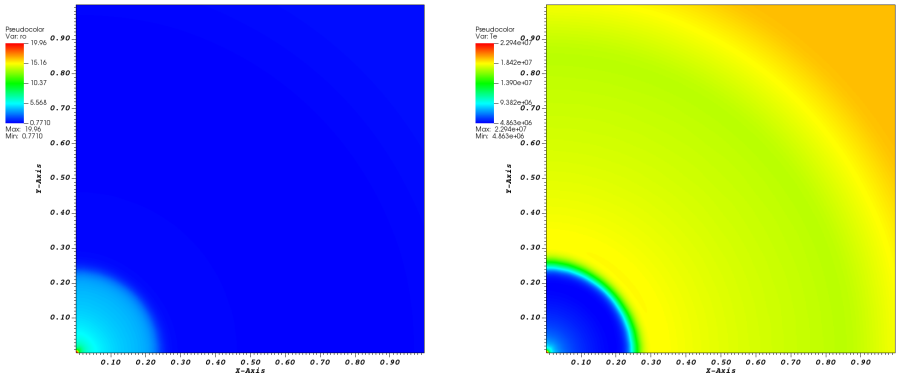

FIGURE 5. Implosion test case with ν_{ei} given by the NRL formulary with a grid of 500 by 500 points. Left: isovalues of the density when the peak occurs. Right: isovalues of the electronic and ionic temperatures when the peak occurs.

When the shock front reaches the center, a peak of density occurs. This peak occurs at time $t = 8.798 \times 10^{-7}$sec. in the monoatomic case, while it occurs here at time $t = 9.2 \times 10^{-7}$sec., see Figure 4. The temperatures are also maximal at the center when this peak occurs, as shown in Figure 5.

REFERENCES

[1] R. Abgrall and S.Karni, A comment on the computation of non-conservative products, *J. Comput. Phys.*, **229** (2010), 2759–2763.

[2] P. Andries, P. Le Tallec, J.-P. Perlat and B. Perthame, Entropy condition for the ES BGK model of Boltzmann equation for mono and polyatomic gases, *Eur. J. Mech. B Fluids*, **19** (2000), 813–830.

[3] D. Aregba-Driollet, J. Breil, S. Brull, B. Dubroca and E. Estibals, Modelling and numerical approximation for the nonconservative bitemperature Euler model, *ESAIM Math. Model. Numer. Anal.*, **52** (2018), 1353–1383.

[4] D. Aregba-Driollet and S. Brull, A viscous approximation of the bitemperature Euler system, *Comm. Math. Sci.*, **17** (2019), 1135–1147.

[5] D. Aregba-Driollet, S. Brull and Y.-J. Peng, Global existence of smooth solutions for a non-conservative bitemperature Euler model, *SIAM J. Math. Anal.*, **53** (2021), 1886–1907.

[6] D. Aregba-Driollet, S. Brull and C. Prigent, A discrete velocity numerical scheme for the two-dimensional bitemperature Euler system, *SIAM J. Numer. Anal.*, **60** (2022), 28–51.

[7] D. Aregba-Driollet and R. Natalini, Discrete kinetic schemes for multidimensional systems of conservation laws, *SIAM J. Numer. Anal.*, **37** (2000), 1973–2004.

[8] T. Arima, S. Taniguchi, T. Ruggeri and M. Sugiyama, Monoatomic rarefied gas as a singular limit of polyatomic gas in extended thermodynamics, *Physics letter A*, **337** (2013), 2136–2140.

[9] C. Baranger, M. Bisi, S. Brull and L. Desvillettes, On the Chapman-Enskog asymptotics of mixture of monoatomic and polyatomic rarefied gases, *Kin. Rel. Mod.*, **11** (2018), 821–858.

[10] F. Bernard, A. Iollo and G. Puppo, BGK polyatomic model for rarefied flows, *J. Sci. Comput.*, **78** (2019), 1893–1916.

[11] M. Bisi, R. Monaco and A. J. Soares, A BGK model for reactive mixtures of polyatomic gases with continuous internal energy, *J. Phys. A*, **51** (2018), 125501, 29 pp.

[12] M. Bisi, T. Ruggeri and G. Spiga, Dynamical pressure in a polyatomic gas: Interplay between kinetic theory and Extended Thermodynamics, *Kinet. Relat. Models*, **11** (2018), 71–95.

[13] M. Bisi and G. Spiga, On a kinetic BGK model for slow chemical reactions, *Kinet. Relat. Models*, **4** (2011), 153–167.

[14] M. Bisi and R. Travaglini, A polyatomic model for mixtures for monoatomic and polyatomic gases, *Phys. A*, **547** (2020), 124441, 18 pp.

[15] A. V. Bobylev, M. Bisi, M. Groppi, G. Spiga and I. Potapenko, A general consistent BGK model for gas mixtures, *Kinet. Relat. Models*, **11** (2018), 1377–1393.

[16] C. Borgnakke and P. S. Larsen, Statistical collision model for Monte-Carlo simulation of polyatomic mixtures, *Journ. Comput. Phys.*, **18** (1975), 405–420.

[17] J.-F Bourgat, L. Desvillettes, P. Le Tallec and B. Perthame, Microreversible collisions for polyatomic gases and Boltzmann's theorem, *Eur. Journ. Fluid Mech.*, **13** (1994), 237–254.

[18] A. Bressan, *Hyperbolic Systems of Conservation Laws*, Oxford Lecture Series in Mathematics and its Applications, 20. Oxford University Press, Oxford, 2000.

[19] S. Brull An Ellipsoidal Statistical Model for a monoatomic and polyatomic gas mixture, *Comm. Math. Sci.*, **19** (2021), 2177–2194.

[20] S. Brull, B. Dubroca and C. Prigent, A kinetic approach of the bi-temperature Euler model, *Kinet. Relat. Models*, **13** (2020), 33–61.

[21] S. Brull and J. Schneider On the Ellipsoidal Statistical Model for polyatomic gases, *Cont. Mech. Thermodyn*, **20** (2009), 489–508.

[22] C. Chalons and F. Coquel, Navier-Stokes equations with several independent pressure laws and explicit predictor-corrector schemes, *Numer. Math.*, **101** (2005), 451–478.

[23] F. Coquel and C. Marmignon, Numerical methods for weakly ionized gas, *Astrophysics and Space Science*, **260** (1998), 15–27.

[24] G. Dal Maso, P. G. Le Floch and F. Murat, Definition and weak stability of nonconservative products, *J. Math. Pures et Appl.*, **74** (1995), 483–548.

[25] L. Desvillettes, Sur un modèle de type Borgnakke-Larsen conduisant à des lois d'énergie non-linéaires en température pour les gas parfaits polyatomiques, *Ann. Fac. Sci. Toulouse Math.*, **6** (1997), 257–262.

[26] L. Desvillettes, R. Monaco and F. Salvarani, A kinetic model allowing to obtain the energy law of polytropic gases in the presence of chemical reactions, *Eur. J. Mech. B Fluids*, **24** (2005), 219–236.

[27] A. Ern and V. Giovangigli, The kinetic equilibrium regime, *Physica A*, **260** (1998), 49–72.

[28] E. Estibals, H. Guillard and A. Sangam, Derivation and numerical approximation of two-temperature Euler plasma model, *J. Comput. Phys.*, **444** (2021), 110565, 48 pp.
[29] H. Funagane, S. Takata, K. Aoki and K. Kugimoto, Poiseuille flow and thermal transpiration of a rarefied polyatomic gas through a circular tube with applications to microflows, *Boll. Unione Mat. Ital.*, **4** (2011), 19–46.
[30] V. Giovangigli, *Multicomponent Flow Modeling. Modeling and Simulation in Science, Engineering and Technology*, Birkhäuser Boston, Inc., Boston, MA, 1999.
[31] B. Graille, T. Magin and M. Massot, Kinetic theory of plasmas, *Maths models and methods in the Appl. Sci.*, **19** (2009), 527–599.
[32] J. M. Greene, Improved Bhatnagar-Gross-Krook model of electron-ion collisions, *Phys.Fluids*, **16** (1973), 2022–2023.
[33] J. D. Huba, *NRL Plasma Formulary*, Revised 2013 version, NRL.
[34] C. Klingenberg, M. Pirner and G. Puppo, A consistent kinetic model for a two-component mixture of polyatomic molecules, *Comm. in Math. Sci.*, **17** (2019), 149–173.
[35] S. Kosuge, K. Aoki and T. Goto, Shock wave structure in polyatomic gases: Numerical analysis using a model Boltzmann equation, *AIP Conf. Proc.*, **1786** (2016), 180004.
[36] C. Pares, Numerical methods for nonconservative hyperbolic systems: A theoretical framework, *SIAM J. Numer. Anal.*, **44** (2006), 300–321.
[37] B. Perthame and C. Simeoni, A kinetic scheme for the Saint-Venant system with a source term, *Calcolo*, **38** (2001), 201–231.
[38] S. Takata, H. Funagane and K. Aoki, Fluid modeling for the Knudsen compressor: Case of polyatomic gases, *Kinet. Relat. Models*, **3** (2010), 353–372.
[39] Q. Wargnier, S. Faure, S. B. Graille, T. Magin and M. Massot, Numerical treatment of the nonconservative product in a multiscale fluid model for plasmas in thermal nonequilibrium: Application to solar physics, *SIAM J. Sci. Comput.*, **42** (2020), B492–B519.
[40] B. Zel'dovich and P. Raizer, *Physics of Shock Waves and High-Temperature Hydrodynamic Phenomena*, Academic Press, 1966.

Received April 2021; revised January 2022; early access April 2022.

E-mail address: denise.aregba@math.u-bordeaux.fr
E-mail address: stephane.brull@math.u-bordeaux.fr